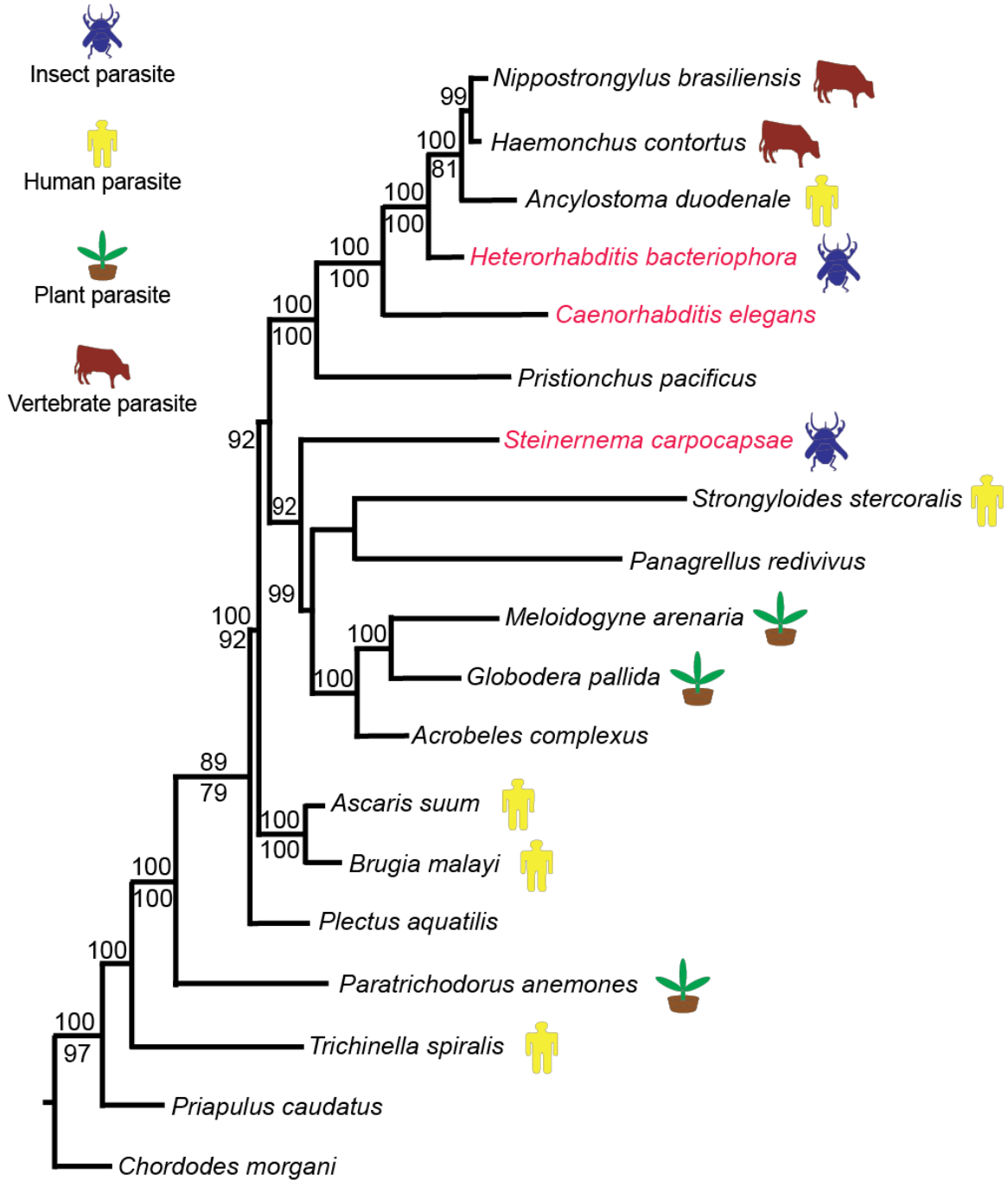


## **Appendix A: Supplementary Materials for Chapter 3\***

---

\*This appendix is available as supplementary material for the published manuscript in *Current Biology* in 2011.

**PARASITE KEY:**

**Figure 3.S1 | Phylogenetic relationships of 17 well-studied or representative species within Nematoda.**

Relationships are based on ML and Bayesian analyses of nearly complete SSU sequences. Values above each branch represent Bayesian posterior probabilities; ML bootstrap indices (1000 replicates) appear below each branch. Values lower than 75 are not reported. Both analyses

produced concordant tree topologies. The ecologies of parasitic taxa are represented by colored icons. *Priapulid* (a priapulid) and *Chordodes* (a nematomorph) were defined as outgroups.

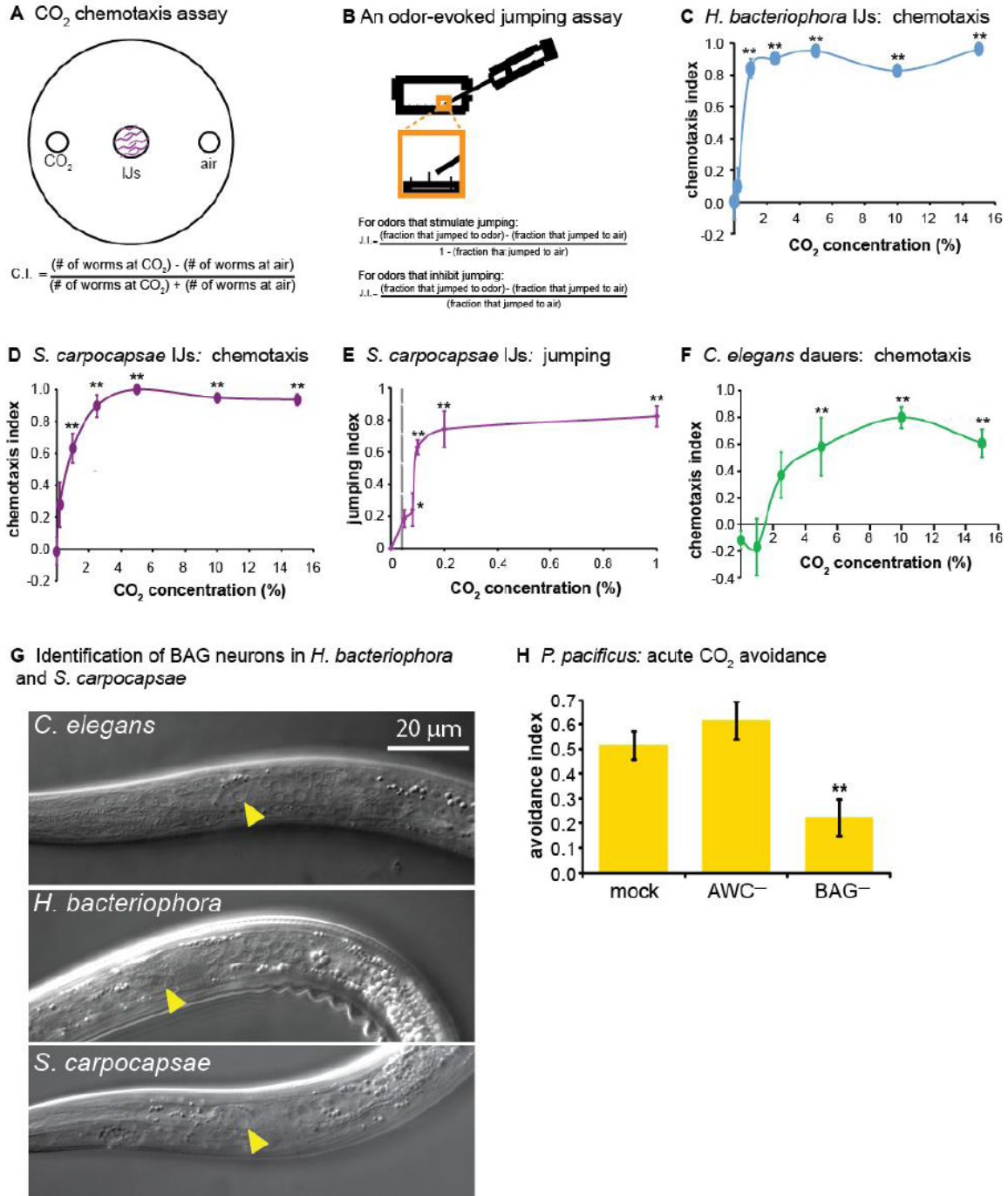
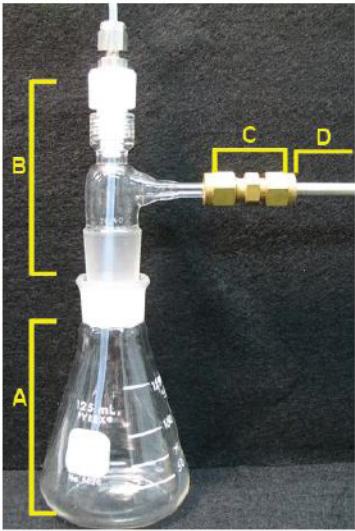


**Figure 3.S2 | CO<sub>2</sub> response across species.** A. The CO<sub>2</sub> chemotaxis assay. Nematodes are

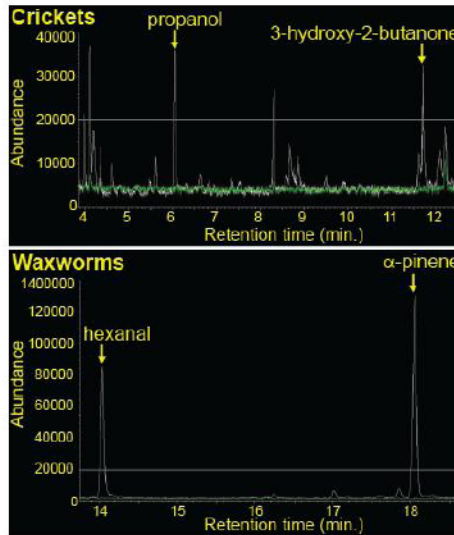
placed in the center of the plate, and allowed to distribute in the CO<sub>2</sub> gradient. The number of worms in each scoring region is then counted. Inner boundaries of scoring regions are indicated by the horizontal lines. The chemotaxis index (C.I.) is calculated as indicated (bottom). **B.** The odor-evoked jumping assay. Individual or populations of nematodes are placed on a piece of filter paper inside a Petri dish. A non-beveled syringe with an attached needle is brought to within 2 mm of an individual nematode that is standing, and a small puff of stimulus is delivered. The percentage of animals that jump within 8 sec. is scored. A jumping index (J.I.) is then calculated as indicated (right) such that the J.I. is normalized to a scale of -1 to +1. The orange box shows an enlarged view of the standing IJ and stimulus syringe. **C–D.** *H. bacteriophora* and *S. carpocapsae* IJs are attracted to CO<sub>2</sub> across concentrations. n = 6–12 trials. **E.** CO<sub>2</sub> also stimulates jumping in *S. carpocapsae* IJs at concentrations as low as 0.08%. The atmospheric concentration of CO<sub>2</sub> (0.04%) is indicated by the dashed line. Saturation was achieved at 0.1% CO<sub>2</sub>; CO<sub>2</sub> concentrations of 0.1% to 15% evoked similar levels of jumping (data not shown). The jumping index was calculated as described in Figure S2B. n = 3–7 trials; for each trial, ~ 60 individual IJs were tested. **F.** *C. elegans* dauers are attracted to CO<sub>2</sub>. n = 5–10 trials. For **C–F**, \*,  $P < 0.05$ ; \*\*,  $P < 0.01$ , one-way ANOVA with Dunnett's post-test. **G.** Identification of BAG neurons in *H. bacteriophora* and *S. carpocapsae*. Nomarski images of the left side of a *C. elegans* larva and parasitic IJs. Arrowheads indicate left BAG neurons. Anterior is to the left; dorsal is up. In *C. elegans* as well as the parasites, BAG neuron cell bodies are located laterally within the body just anterior to the nerve ring. **H.** BAG neurons are required for acute CO<sub>2</sub> avoidance in the necromenic nematode *Pristionchus pacificus*. The acute assay for CO<sub>2</sub> avoidance was performed as previously described [1]. The avoidance index was calculated as a.i. = (fraction of worms that reversed in response to CO<sub>2</sub>)—(fraction of worms that reversed in response to air control). n = 17–19 worms for each treatment. \*\*,  $P < 0.01$ , Fisher's exact test. For all graphs, error bars represent SEM. We note that for all experiments, assay chambers were open to the external

environment; thus the same ambient level of CO<sub>2</sub> (~ 0.04%) was present in all experiments.

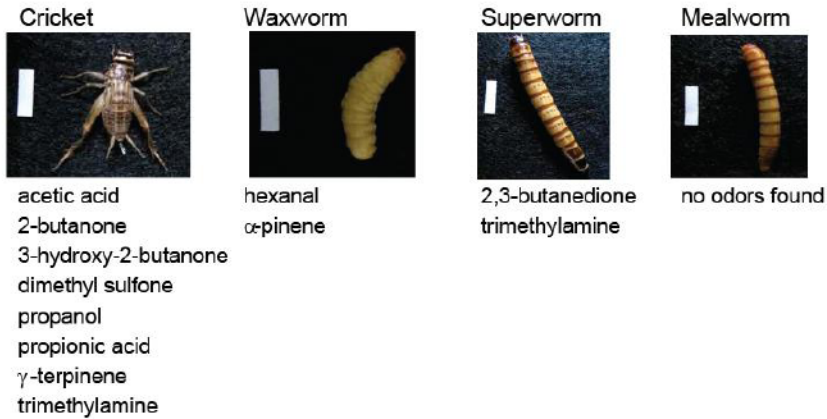
### A Setup for sampling insect headspace



### B Chromatograph snapshots



### C Odors found in insect headspace



### D Soda lime blocks attraction to CO<sub>2</sub>

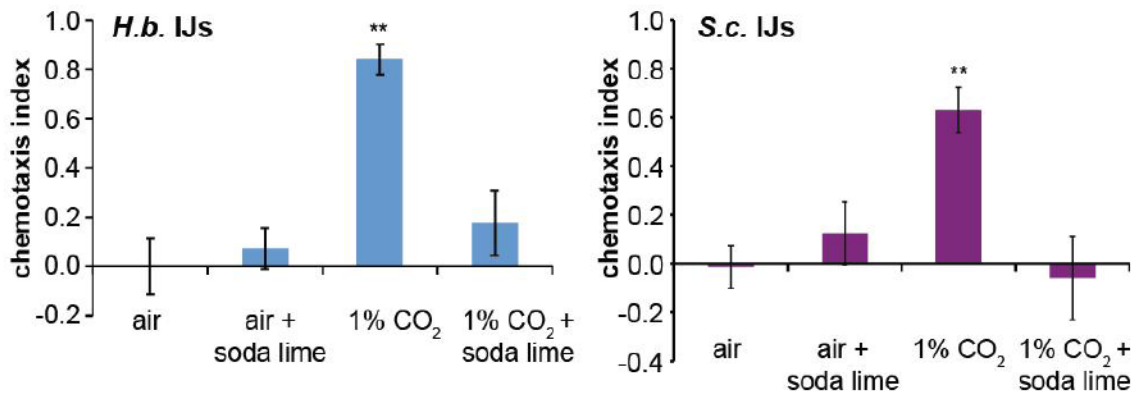
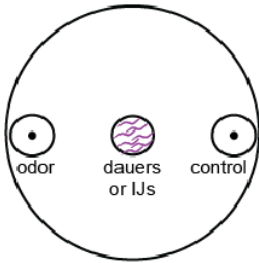


**Figure 3.S3 | Identification of insect volatiles by TD-GC-MS. A.** Little is known about

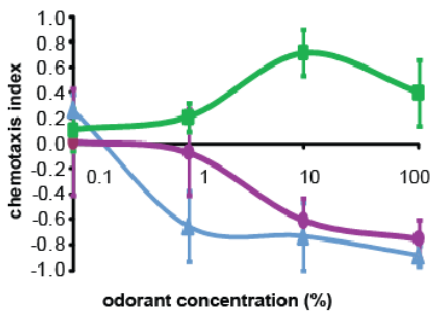
the odorants emitted by insect larvae. We therefore performed TD-GC-MS to identify odorants emitted by three species of insect larvae (*Galleria mellonella*, *Zophobas morio*, and *Tenebrio molitor*), as well as young adult crickets (*Acheta domesticus*). **A.** The unit used to sample insect headspace. (A) is a 125 ml glass Erlenmeyer flask. (B) is a hand-blown glass adaptor with a ground glass attachment fit into the flask, a Teflon top piece fit to accommodate a 1/8" O.D. Teflon tube for air flow, and a small side neck tapered to 1/4" O.D. (C) is a 1/4" female/female Swagelok compression fitting for the attachment of the thermal desorption tube to the flask, where air and any volatiles flow out of the set-up. (D) is the thermal desorption tube. For each species, six experimental replicates and three control replicates were obtained. The number of insects sampled in each run, and the average population weights ( $\pm$  SEM), are as follows: *A. domesticus*: 50 insects, 8.64 g ( $\pm$  0.15); *G. mellonella*: 100 insects, 28.89 g ( $\pm$  2.79); *Z. morio*: 40 insects, 27.48 g ( $\pm$  0.65); *T. molitor*: 50 insects, 17.0 g ( $\pm$  0.61). Control samples did not contain insects. **B.** Representative snapshots of the ion chromatograph data acquired from cricket (upper trace) and waxworm (lower trace) headspace. White traces represent insect headspace samples and green traces represent controls. Compounds identified in multiple traces at relative abundances of  $\geq 20,000$ , and that were not present in the controls at detectable levels, were then positively identified. Compounds meeting these criteria are indicated with yellow arrows. **C.** Compounds identified from the four insect species tested. Scale bars in insect photographs are 1 cm x 2.5 mm. **D.** A soda lime assay for examining the responses to host volatiles besides CO<sub>2</sub>. The assay is a modified version of the host chemotaxis assay in which the airstream containing host volatiles is passed through a column of soda lime before entering the assay plate. As a control, here we show that for both *H. bacteriophora* IJs (left graph) and *S. carpocapsae* IJs (right graph), soda lime alone does not elicit a behavioral response and passing an airstream containing 1% CO<sub>2</sub> through a column of soda lime eliminates the attractive response to CO<sub>2</sub>. Thus, a soda lime column can be used to chemically remove CO<sub>2</sub> from an airstream. n = 8–16 trials. \*\*,  $P < 0.01$ , one-way ANOVA with Dunnett's post-test.

**A Chemotaxis assay**

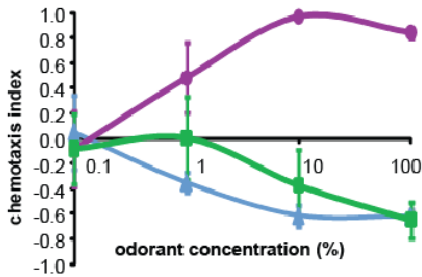


**B Chemotaxis across species**

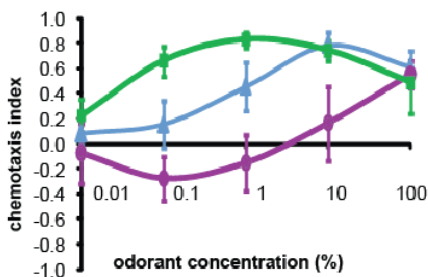
Responses to 2,3-butanedione



Responses to 1-heptanol



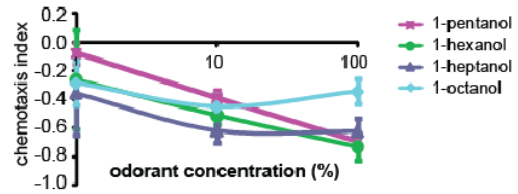
Responses to 4,5-dimethylthiazole



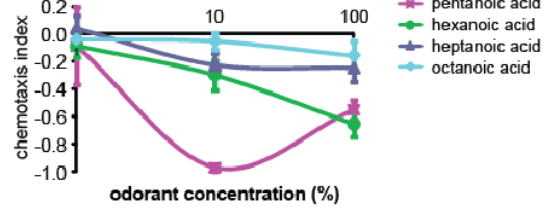
— *C. elegans* dauers  
 — *H. bacteriophora* IJs  
 — *S. carpocapsae* IJs

**C Chemotaxis by *H. bacteriophora* IJs**

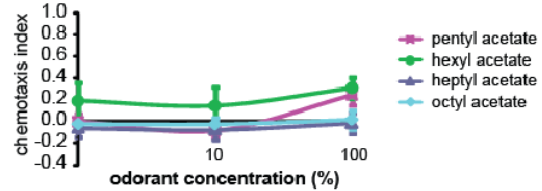
Response to alcohols



Response to acids

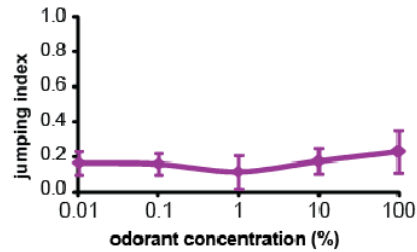


Response to acetates

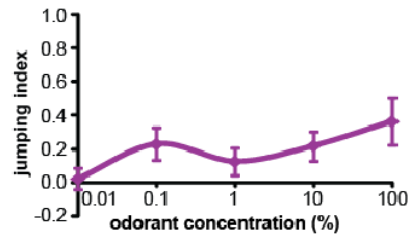


**D Jumping by *S. carpocapsae* IJs**

Response to 1-heptanol



Response to  $\alpha$ -pinene



Response to 2,3-butanedione

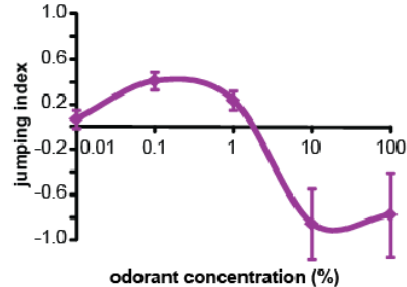


**Figure 3.S4 | Dose-response analysis across species.** **A.** A schematic of the chemotaxis assay. Nematodes are placed in the center of the plate, and allowed to distribute in the odor gradient. After three hours, the number of worms in each scoring region is counted. Scoring regions are indicated by the circles at either side of the plate. The chemotaxis index (C.I.) is then calculated as indicated (bottom). **B.** Responses to increasing concentrations of 2,3-butanedione, 1-heptanol, and 4,5-dimethylthiazole in a chemotaxis assay.  $n = 5\text{--}33$  trials. **C.** Responses of *H. bacteriophora* to alcohols, acids, and acids.  $n = 5\text{--}33$  trials. Error bars represent SEM. Responses to 1-heptanol are from **B.** **D.** Jumping responses of *S. carpocapsae* to increasing concentrations of 1-heptanol,  $\alpha$ -pinene, and 2,3-butanedione in a jumping assay.  $n = 3\text{--}8$  trials; for each trial,  $\sim 60$  individual IJs were tested. For all graphs, error bars represent SEM.

**Table 3.S1 | Odorants tested in chemotaxis and jumping assays.** Odorants were selected based on their chemical diversity and ecological relevance. All of the odorants tested are present either in plants or bacteria [2–5], and many have been shown to elicit responses from free-living adult nematodes [6–9]. Eleven of the odorants were identified in insect headspace (Figure 2.S7). In addition, hexadecanoic and octadecanoic acid have been identified in larval cuticular extracts from insect larvae [10]; acetic, propionic, and pentanoic acids have been identified in cricket excreta [11]; benzaldehyde and linalool have been identified in butterfly wing extracts [12]; and nonanal, undecanal, and nonanol are emitted by adult wax moths [13, 14]. Product numbers are from Sigma-Aldrich, except for ethanol (Pharmco-AAPER), ethyl acetate (Mallinckrodt chemicals), and acetic acid (J.T. Baker).

	<i>C. elegans</i>			<i>H. bacteriophora</i>			<i>S. carpocapsae</i>					
	C.I.	n	SEM	C.I.	n	SEM	C.I.	n	SEM	J.I.	n	SEM
ethanol	0.33	5	0.21	-0.22	5	0.12	-0.06	5	0.09	-1.00	3	0.30
1-propanol	0.51	5	0.22	0.36	5	0.13	-0.28	5	0.21	-1.00	3	0.30
1-pentanol	-0.24	7	0.27	-0.66	15	0.06	0.39	5	0.10	-0.92	4	0.31
1-hexanol	-0.61	7	0.27	-0.73	22	0.04	0.83	6	0.08	-0.50	4	0.42
1-heptanol	-0.65	10	0.14	-0.62	33	0.05	0.84	8	0.04	0.16	8	0.10
1-octanol	-0.88	5	0.08	-0.34	15	0.07	0.48	5	0.14	0.24	9	0.12
1-nonanol	-0.79	5	0.11	-0.62	5	0.11	0.53	6	0.08	0.24	8	0.61
isopropyl alcohol	0.18	5	0.29	-0.39	5	0.22	-0.03	5	0.22	-0.68	3	0.43
isoamyl alcohol	0.29	7	0.24	-0.21	5	0.15	-0.05	5	0.05	0.06	6	0.09
linalool	0.38	5	0.14	-0.05	6	0.23	-0.09	5	0.28	0.12	6	0.10
methyl acetate	0.64	5	0.15	-0.38	5	0.09	0.11	5	0.11	-0.71	3	0.34
ethyl acetate	0.36	5	0.23	-0.16	15	0.10	0.26	5	0.13	-0.89	3	0.31
pentyl acetate	-1.00	5	0.00	0.26	13	0.09	-0.09	6	0.10	-1.00	3	0.30
hexyl acetate	-0.70	5	0.29	0.31	5	0.10	0.08	6	0.09	-0.01	8	0.64
heptyl acetate	-0.80	5	0.20	-0.02	14	0.09	0.33	5	0.17	0.08	8	0.10
octyl acetate	-0.37	6	0.31	0.01	14	0.09	0.49	5	0.14	0.37	8	0.14
nonyl acetate	-0.01	5	0.16	-0.25	5	0.15	0.15	5	0.04	0.24	10	0.12
decyl acetate	-0.40	5	0.19	0.10	5	0.20	0.08	5	0.09	-0.89	3	0.31
dodecyl acetate	0.19	5	0.17	0.45	5	0.10	-0.02	6	0.09	0.22	8	0.11
2-butanone	0.83	5	0.11	0.02	6	0.13	-0.18	5	0.24	-0.66	3	2.39
2-pentanone	0.67	5	0.13	-0.29	5	0.13	-0.39	5	0.07	-0.46	5	0.46
2-hexanone	-0.50	5	0.22	-0.36	7	0.15	0.11	5	0.09	-0.89	3	0.31
2-heptanone	-0.99	5	0.01	0.19	5	0.23	0.18	5	0.24	-0.68	3	0.35
2-octanone	-1.00	5	0.00	0.11	5	0.15	0.30	5	0.24	-0.68	3	0.43
2-nonanone	-0.95	5	0.04	0.05	5	0.19	0.52	5	0.12	-0.89	3	0.31
2,3-butanedione	0.40	5	0.26	-0.89	5	0.08	-0.75	5	0.15	-0.89	6	0.31
3-hydroxy-2-butanone	0.25	5	0.12	-0.23	5	0.06	-0.17	5	0.05	-0.74	3	0.33
dimethyl sulfone	0.02	5	0.25	0.00	6	0.19	-0.18	5	0.06	0.16	3	0.09
acetic acid	-1.00	6	0.00	-0.66	8	0.23	-0.98	5	0.02	-0.73	3	0.33
propionic acid	-1.00	5	0.00	-1.00	5	0.00	-1.00	5	0.00	0.43	3	0.06
pentanoic acid	-1.00	5	0.00	-0.55	7	0.07	-0.80	5	0.20	0.46	9	0.10
hexanoic acid	-1.00	5	0.00	-0.66	14	0.09	-0.43	7	0.18	0.42	8	0.11
heptanoic acid	-0.90	5	0.10	-0.25	17	0.10	-0.46	5	0.13	0.07	8	0.09
octanoic acid	-0.78	5	0.13	-0.16	14	0.10	-0.53	5	0.19	-0.47	6	0.34
nonanoic acid	-0.68	5	0.19	-0.33	5	0.20	-0.17	5	0.11	0.21	8	0.10
hexadecanoic acid	0.12	5	0.14	-0.06	7	0.24	-0.15	5	0.24	-1.00	3	0.30
octadecanoic acid	0.36	5	0.15	-0.16	5	0.11	-0.02	5	0.20	-1.00	3	0.30
hexanal	-0.70	5	0.14	-0.75	7	0.20	-0.31	7	0.20	0.30	10	0.10
nonanal	-0.45	6	0.06	-0.01	5	0.24	0.09	5	0.10	0.37	9	0.11
undecanal	-0.71	5	0.19	0.24	5	0.16	-0.09	5	0.17	0.01	4	0.06
2-acetylthiazole	0.03	5	0.34	-0.73	8	0.04	-0.15	5	0.25	-0.79	3	0.31
benzothiazole	0.71	5	0.12	-0.06	8	0.05	-0.49	5	0.18	-0.40	6	0.37
2-isobutylthiazole	-0.76	5	0.12	-0.04	8	0.09	-0.04	5	0.29	0.07	8	0.09
4,5-dimethylthiazole	0.49	7	0.25	0.61	6	0.12	0.55	5	0.11	-1.00	6	0.30
benzaldehyde	-0.75	5	0.14	-0.83	5	0.08	0.07	5	0.11	-0.53	5	0.43
methyl salicylate	-0.93	5	0.03	0.86	5	0.02	0.07	5	0.17	-0.79	3	0.36
m-xylene	-0.04	5	0.22	-0.45	5	0.21	-0.05	5	0.03	0.07	6	0.11
m-cymene	-0.04	5	0.17	0.19	7	0.23	-0.10	5	0.17	0.03	5	0.06
p-cymene	-0.30	5	0.20	0.41	5	0.22	-0.10	5	0.07	0.02	8	0.09
$\beta$ -caryophyllene	0.27	5	0.24	0.06	10	0.07	-0.40	5	0.13	-0.89	3	0.31
$\alpha$ -humulene	0.45	7	0.27	0.00	5	0.25	0.30	5	0.20	-0.04	3	0.30
3-carene	0.48	5	0.25	-0.70	5	0.07	-0.13	6	0.05	-0.89	3	0.31
$\alpha$ -pinene	0.57	5	0.17	-0.63	5	0.12	0.05	5	0.21	0.36	8	0.14
$\beta$ -pinene	0.30	5	0.17	-0.17	5	0.11	-0.17	5	0.25	0.23	6	0.10
limonene	0.16	5	0.14	-0.64	5	0.12	-0.35	5	0.07	-0.50	5	0.30
$\gamma$ -terpinene	0.13	7	0.24	-0.02	5	0.14	-0.12	5	0.12	0.26	8	0.10
trimethylamine	0.75	5	0.08	-0.28	5	0.14	0.12	7	0.25	-0.03	3	0.36

**Table 3.S1** | Mean values for the chemotaxis index (C.I.) and jumping index (J.I.) of each species in response to each tested stimulus. The number of trials (n) is shown. SEM, standard error of the mean. Odorants were selected based on their chemical diversity and ecological relevance. All of the odorants tested are present either in plants or bacteria [2–5], and many have been shown to elicit responses from free-living adult nematodes [6–9]. Eleven of the odorants were identified in insect headspace (Figure 5). In addition, hexadecanoic and octadecanoic acid have been identified in larval cuticular extracts from insect larvae [10]; acetic, propionic, and pentanoic acids have been identified in cricket excreta [11]; benzaldehyde and linalool have been identified in butterfly wing extracts [12]; and nonanal, undecanal, and nonanol are emitted by adult wax moths [13, 14]. Product numbers are from Sigma-Aldrich, except for ethanol (Pharmco-AAPER), ethyl acetate (Mallinckrodt chemicals), and acetic acid (J.T. Baker).

### Supplemental Methods

**Nematodes.** *H. bacteriophora* were from the inbred strain M31e [15, 16], *S. carpocapsae* were from the inbred strain ALL [17], and *C. elegans* were from the standard N2 (“Bristol”) strain, unless otherwise indicated. Other *H. bacteriophora* strains tested were HP88 [18], GPS11 [19], NC1 [20], and a strain we designate as “BU” that was derived from commercially available nematodes that were originally obtained from Becker-Underwood (<http://www.beckerunderwood.com>). The other *S. carpocapsae* strain tested was an inbred wild isolate that we designate as Base [17]. Other *C. elegans* strains tested were the wild isolate CB4856 (“Hawaii”) and CX11697 [*kyIs536[flp-17::p17::s12GFP, elt-2::mCherry]*; *kyIs538[glb-5::p12::s12GFP, elt-2::mCherry]*], which contains a genetic ablation of the BAG neurons. *P. pacificus* were from the PS312 (“California”) strain.

**Nematode culture.** *H. bacteriophora* was cultured at 27°C on either nutrient agar + cholesterol plates (23 g nutrient agar + 1 ml of 5 mg/ml cholesterol in 1 L) or lipid agar +

cholesterol plates [21] seeded with either TT01 or RET16 bacteria. RET16 is a GFP-labeled derivative of *P. temperata* strain NC1 mutated with HiMarGM (a hyperactive mariner transposon with gentamicin resistance) [15]. *Photorhabdus* was grown in PP3 broth (20 g proteose peptone #3 (Difco) in 1 L dH<sub>2</sub>O) and on either nutrient agar + cholesterol plates or lipid agar + cholesterol plates. IJs were stored in 0.85% NaCl (w/v) or dH<sub>2</sub>O at room temperature or 15°C prior to use. Prior to behavioral testing, IJs were washed in dH<sub>2</sub>O. For Figure 1A, *H. bacteriophora* was cultured on plates seeded with GFP-labeled *P. luminescens*, as previously described [16].

*S. carpocapsae* was cultured as previously described [22]. Briefly, 5 last-instar *Galleria mellonella* larvae (American Cricket Ranch, Lakeside, CA) were placed in a 5 cm Petri dish with a 55 mm Whatman 1 filter paper acting as a pseudo-soil substrate in the bottom of the dish.  $\leq 250 \mu\text{l}$  containing 500–1000 IJs suspended in water was evenly distributed on the filter paper. After 7–10 days the insect cadavers were placed on White traps [23]. Emerging IJs were harvested, washed for 10 minutes in 0.4% Hyamine 1622 solution (Fluka), and rinsed 3 times with water. To prevent differences in inbreeding between batches of IJs, the same stock population of IJs was used to generate all test batches of IJs. Stock populations were stored at 15°C and propagated in *G. mellonella* every 10 days to produce fresh test batches of IJs. Test batches were stored at room temperature and used in behavioral assays within 12 days of emergence. In some cases, *S. carpocapsae* used for chemotaxis assays were cultured at 27°C on nutrient agar + cholesterol or lipid agar + cholesterol plates as described above, except that plates were seeded with *X. nematophila* strain HGB081 [24]. For Figure 1B, *S. carpocapsae* were cultured on plates seeded with GFP-labeled *X. nematophila*, as previously described [25]. *X. nematophila* was grown in LB broth containing 0.1% sodium pyruvate, and on either nutrient agar + cholesterol or lipid agar + cholesterol plates.

*C. elegans* was cultured on NGM plates seeded with *E. coli* OP50 according to standard methods [26]. *C. elegans* dauers were grown primarily in liquid culture, although in some cases dauers were collected from the lids of starved plates. For dauers grown in liquid culture, embryos were collected as previously described and diluted to 10 eggs/ml in

S complete media [27]. *E. coli* HB101 bacteria was added at a final concentration of 0.5 mg/ml and worms were grown on a carousel at 20°C for 6 days to generate dauers (L.R. Baugh and P.W. Sternberg, unpublished). If necessary, the bacterial concentration was adjusted to generate populations of nearly 100% dauers. Dauers were stored in dH<sub>2</sub>O at 15°C prior to use. For CO<sub>2</sub> assays, dauers were SDS-treated [28]; SDS treatment did not affect CO<sub>2</sub> response. For all other assays, dauers were not treated with SDS; in these cases, a small population sample was treated with SDS, and worms were only used for behavioral assays if nearly all of the sample population survived SDS treatment.

*P. pacificus* was grown on NGM plates seeded with *E. coli* OP50 bacteria at room temperature.

**Phylogenetic analysis.** Small subunit ribosomal DNA (SSU rDNA) sequences for all analyses were obtained from GenBank for all taxa included in the present study (accession numbers: AJ920356, AJ920348, AJ417024, EU086375, AF036593, AY268117, U81584, AF083007, AF279916, AF036604, AY284620, AY284621, AY284671, U94367, AF036588, U61761, AF036600, U60231, EU344798, X87984, and AF036639). Most of these sequences have been used in previous phylogenetic analyses [29, 30]. The SSU sequences for *C. elegans*, *S. carpocapsae*, *H. bacteriophora*, and *C. morgani* (a nematomorph) were used for the neighbor-joining (NJ) tree in Figure 4C. The sequences were first trimmed to 1783 characters and then aligned using MUSCLE [31]. The subsequent NJ analysis was done using the ‘Dnadist’ and ‘Neighbor’ programs from the PHYLIP 3.68 package [32] using default settings with *C. morgani* defined as the outgroup. A total of 19 nematode species and 2 outgroup taxa (a priapulid and a nematomorph) were used in the analyses for Figure S1. In order to facilitate comparison of the SSU sequences of varying lengths, the ends were trimmed by hand, prior to alignment, in MacClade 4 [33] to a maximum length of 1152 characters, which is the length of the taxon with the shortest sequence, *Parastrongyloides trichosuri*. Sequences were then aligned using MUSCLE [31], resulting in 1313 characters (including gaps). The TIM2+I+G model was selected as the best-fit model of substitution for all analyses using the AIC and AICc model selection criteria in the program jModelTest [34, 35].

Maximum likelihood and bootstrap (1000 replicates) analyses were carried out in PhyML 3.0 [35] using the parameters for base frequencies, substitution rate matrix, proportion of invariable sites, number of substitution categories, and shape distribution parameter determined as the best-fit by jModelTest (freqA = 0.2684, freqC = 0.1835, freqG = 0.2501, freqT = 0.2981, Ra(AC) = 1.6751, Rb(AG) = 2.5642, Rc(AT) = 1.6751, Rd(CG) = 1.0000, Re(CT) = 4.5613, Rf(GT) = 1.0000, p-inv = 0.1710, and gamma shape = 0.5840). Bayesian analysis was carried out using MrBayes 3.1.2 [36]. The number of substitution categories, substitution rate matrix, shape and proportion of invariant sites were based on the parameters determined by jModelTest (as above). The parameters for base frequencies and relative rates were allowed to vary throughout the analysis. The parameters were unlinked to allow for more flexibility in searching tree space. Trees were sampled every 1000 generations. The burn-in value was set to 2000 trees. The total number of generations was set to 8 million. Four parallel chains (one cold and three heated) were used. A majority-rule consensus tree was reconstructed after discarding the burn-in.

#### **Thermal desorption-gas chromatography-mass spectrometry (TD-GC-MS).**

Appropriately staged insects (adult *Acheta domesticus* and last-instar larvae of *Zophobas morio*, *Galleria mellonella*, and *Tenebrio molitor*) were placed in a 125 ml glass beaker and sampled for 30 minutes with a stream of air (10% oxygen, 90% nitrogen) flowing into the flask and out through a thermal desorption tube (Sigma-Aldrich 20913-U) at a flow rate of approximately 104 ml/min. Experiments were done in pairs and replicated 3 times, with an empty control flask being run each time. To prevent carry-over of odors between experiments, all tubing used was Nalgene Teflon tubing, connected with Swagelok compression fittings, and flasks were cleaned and sterilized after each use.

The contents of the thermal desorption tubes were transferred to a HP 6890 GC–5973 MS system (Agilent Technologies, US) with an Eclipse 4660 purge and trap sampler equipped with an airtube desorber accessory (OI Analytical, College Station, TX, US.). Tubes were desorbed at 200°C for 15 minutes and transferred via a flow of helium to an internal trap held at room temperature. After desorption, the internal trap was heated

to 200°C. This trap was brought in line with the GC carrier gas flow as the trap reached 180°C. The trap was then taken offline and subjected to a bake-out procedure. The sample flowed to a GC via a transfer line held at 120°C where it entered a split-splitless injector held at 200°C. The injector was operated in split mode with a split ratio of 30:1, and a 1 mm liner was installed to optimize chromatographic resolution. Separation was achieved with a HP-624 capillary column (30 m x 0.320 mm) where a volumetric flow of 1 ml/min was maintained with electronic pressure control. The transfer line to the mass spectrometer was held at 200°C, the ion source at 250°C and the quadrupole at 100°C. The mass spectrometer is equipped with an electron impact source. Electron energy was set to 70 eV to obtain the best possible library spectrum matches. The quadrupole mass spectrometer was operated with a full width at half maximum of 0.65 m/z. Mass calibration was verified weekly. The GC oven was ramped from 30°C to 260°C and run for 42 minutes. Data was analyzed with both Chemstation and Masshunter software. Mass spectra were searched against the Wiley library (275,000 spectra) of electron impact mass spectra. Only compounds that were found in multiple traces ( $\geq 2$ ), with a relative abundance  $\geq 20,000$ , and not present in the control traces were considered in this study. Compounds identified in this way were then positively confirmed by running the pure compound (Table S1) and comparing the retention time and mass spectra of the assay-identified compound to the known compound. In cases where the retention time was off by  $\geq 0.5$  minutes or the mass spectra did not match, the assay-identified compound was considered uncertain and not used in behavioral assays. All insects tested were obtained from commercial sources (American Cricket Ranch, Lakeside CA).

### **Data Analysis**

Statistical analysis was performed using GraphPad InStat. Heat maps and dendrograms were generated using PAST [37].

### **References**

1. Hallem, E.A., and Sternberg, P.W. (2008). Acute carbon dioxide avoidance in *Caenorhabditis elegans*. *Proc Natl Acad Sci U S A* *105*, 8038–8043.

2. TNO (2004). Volatile compounds in food: qualitative and quantitative data.
3. O'Leary W, M. (1962). The Fatty Acids of Bacteria. *Bacteriol Rev* 26, 421–447.
4. Malo, E.A., Medina-Hernandez, N., Virgen, A., Cruz-Lopez, L., and Rojas, J.C. (2002). Electroantennogram and field responses of *Spodoptera frugiperda* males (Lepidoptera: Noctuidae) to plant volatiles and sex pheromone. *Folia Entomol. Mex.* 41, 329–338.
5. Ali, J.G., Alborn, H.T., and Stelinski, L.L. (2010). Subterranean Herbivore-induced Volatiles Released by Citrus Roots upon Feeding by *Diaprepes abbreviatus* Recruit Entomopathogenic Nematodes. *J. Chem. Ecol.* 36, 361–368.
6. Bargmann, C.I., Hartweg, E., and Horvitz, H.R. (1993). Odorant-selective genes and neurons mediate olfaction in *C. elegans*. *Cell* 74, 515–527.
7. Hong, R.L., and Sommer, R.J. (2006). Chemoattraction in *Pristionchus* nematodes and implications for insect recognition. *Current biology: CB* 16, 2359–2365.
8. Hong, R.L., Svatos, A., Herrmann, M., and Sommer, R.J. (2008). Species-specific recognition of beetle cues by the nematode *Pristionchus maupasi*. *Evolution & development* 10, 273–279.
9. Rasmann, S., Kollner, T.G., Degenhardt, J., Hiltbold, I., Toepfer, S., Kuhlmann, U., Gershenzon, J., and Turlings, T.C. (2005). Recruitment of entomopathogenic nematodes by insect-damaged maize roots. *Nature* 434, 732–737.
10. Golebiowski, M., Malinski, E., Bogus, M.I., Kumirska, J., and Stepnowski, P. (2008). The cuticular fatty acids of *Calliphora vicina*, *Dendrolimus pini* and *Galleria mellonella* larvae and their role in resistance to fungal infection. *Insect Biochem Mol Biol* 38, 619–627.
11. McFarlane, J.E., Steeves, E., and Alli, I. (1983). Aggregation of larvae of the house cricket, *Acheta domesticus* (L.), by propionic acid present in the excreta. *J. Chem. Ecol.* 9, 1307–1315.
12. Honda, K. (1980). Odor of a papilionid butterfly: odoriferous substances emitted by *Atrophaneura alcinous alcinous* (Lepidoptera: Papilionidae). *J. Chem. Ecol.* 6, 867–873.
13. Leyrer, R.L., and Monroe, R.E. (1973). Identification and isolation of the scent of the moth, *Galleria mellonella*, and a revaluation of its sex pheromone. *J. Insect Physiol.* 19, 2267–2271.
14. Romel, K.E., Scott-Dupree, C.D., and Carter, M.H. (1992). Qualitative and quantitative analyses of volatiles and pheromone gland extracts collected from *Galleria mellonella* (L.) (Lepidoptera: Pyralidae). *J. Chem. Ecol.* 18, 1255–1268.

15. Hallem, E.A., Rengarajan, M., Ciche, T.A., and Sternberg, P.W. (2007). Nematodes, bacteria, and flies: a tripartite model for nematode parasitism. *Current biology: CB* 17, 898–904.
16. Ciche, T.A., Kim, K.S., Kaufmann-Daszczuk, B., Nguyen, K.C., and Hall, D.H. (2008). Cell invasion and matricide during *Photorhabdus luminescens* transmission by *Heterorhabditis bacteriophora* nematodes. *Applied and environmental microbiology* 74, 2275–2287.
17. Bilgrami, A.L., Gauger, R., Shapiro-Ilan, D.I., and Adams, B.J. (2006). Source of trait deterioration in entomopathogenic nematodes *Heterorhabditis bacteriophora* and *Steinernema carpocapsae* during *in vivo* culture. *Nematology* 8, 397–409.
18. Poinar, G.O., Jr. (1990). Taxonomy and biology of Steinernematidae and Heterorhabditidae. In *Entomopathogenic Nematodes in Biological Control*, R. Gaugler and H.K. Kaya, eds. (Boca Raton: CRC Press), pp. 23–61.
19. Grewal, P.S., Grewal, S.K., Malik, V.S., and Klein, M.G. (2002). Differences in the susceptibility of introduced and native white grub species to entomopathogenic nematodes from various geographic localities. *Biol. Contr.* 24, 230–237.
20. Stock, S.P., and Kaya, H.K. (1996). A Multivariate Analysis of Morphometric Characters of *Heterorhabditis* Species (Nemata:Heterorhabditidae) and the Role of Morphometrics in the Taxonomy of Species of the Genus. *J. Parasitol.* 82, 806–813.
21. Vivas, E.I., and Goodrich-Blair, H. (2001). *Xenorhabdus nematophilus* as a model for host-bacterium interactions: *rpoS* is necessary for mutualism with nematodes. *J Bacteriol* 183, 4687–4693.
22. Kaya, H.K., and Stock, S.P. (1997). Techniques in insect nematology. In *Manual of techniques in insect pathology*, L. Lacey, ed. (San Diego, CA: Academic Press Limited).
23. White, G.F. (1927). A Method for Obtaining Infective Nematode Larvae from Cultures. *Science* 66, 302–303.
24. Richards, G.R., Vivas, E.I., Andersen, A.W., Rivera-Santos, D., Gilmore, S., Suen, G., and Goodrich-Blair, H. (2009). Isolation and characterization of *Xenorhabdus nematophila* transposon insertion mutants defective in lipase activity against Tween. *J Bacteriol* 191, 5325–5331.
25. Martens, E.C., Heungens, K., and Goodrich-Blair, H. (2003). Early colonization events in the mutualistic association between *Steinernema carpocapsae* nematodes and *Xenorhabdus nematophila* bacteria. *J Bacteriol* 185, 3147–3154.
26. Brenner, S. (1974). The genetics of *Caenorhabditis elegans*. *Genetics* 77, 71–94.

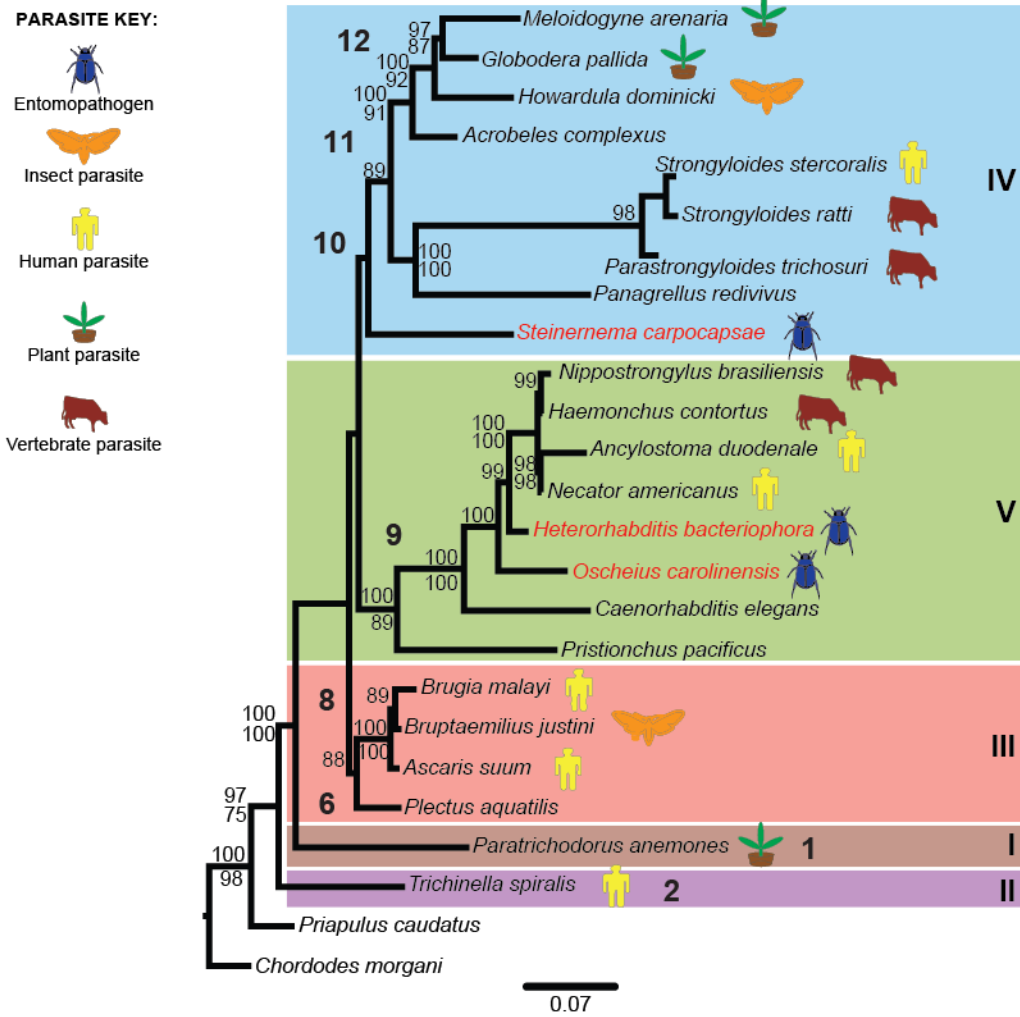
27. Lewis, J.A., and Fleming, J.T. (1995). Basic culture methods. In *Caenorhabditis elegans: Modern Biological Analysis of an Organism*, Volume 48, H.F. Epstein and D.C. Shakes, eds. (San Diego: Academic Press), pp. 4–27.
28. Cassada, R.C., and Russell, R.L. (1975). The dauerlarva, a post-embryonic developmental variant of the nematode *Caenorhabditis elegans*. *Dev Biol* 46, 326–342.
29. Blaxter, M.L., De Ley, P., Garey, J.R., Liu, L.X., Scheldeman, P., Vierstraete, A., Vanfleteren, J.R., Mackey, L.Y., Dorris, M., Frisse, L.M., et al. (1998). A molecular evolutionary framework for the phylum Nematoda. *Nature* 392, 71–75.
30. Meldal, B.H., Debenham, N.J., De Ley, P., De Ley, I.T., Vanfleteren, J.R., Vierstraete, A.R., Bert, W., Borgonie, G., Moens, T., Tyler, P.A., et al. (2007). An improved molecular phylogeny of the Nematoda with special emphasis on marine taxa. *Molecular phylogenetics and evolution* 42, 622–636.
31. Edgar, R.C. (2004). MUSCLE: a multiple sequence alignment method with reduced time and space complexity. *BMC Bioinformatics* 5, 113.
32. Felsenstein, J. (1989). PHYLIP—Phylogeny Inference Package (Version 3.2). *Cladistics* 5, 164–166.
33. Maddison, W.P., and Maddison, D.R. (1989). Interactive analysis of phylogeny and character evolution using the computer program MacClade. *Folia Primatol (Basel)* 53, 190–202.
34. Posada, D. (2009). Selection of models of DNA evolution with jModelTest. *Methods Mol Biol* 537, 93–112.
35. Guindon, S., and Gascuel, O. (2003). A simple, fast, and accurate algorithm to estimate large phylogenies by maximum likelihood. *Syst Biol* 52, 696–704.
36. Huelsenbeck, J.P., and Ronquist, F. (2001). MRBAYES: Bayesian inference of phylogenetic trees. *Bioinformatics* 17, 754–755.
37. Hammer, Ø., Harper, D.A.T., and Ryan, P.D. (2001). PAST: Paleontological Statistics Software Package for Education and Data Analysis. *Palaeontol Electronica* 4, 9.

## **Appendix B: Supplementary Materials for Chapter 4\***

---

\*This appendix is available as supplementary material for the published manuscript in *PNAS* in 2012.

**A** Phylogeny of selected nematode species



**B** Phylogeny of selected *Steinernema* species

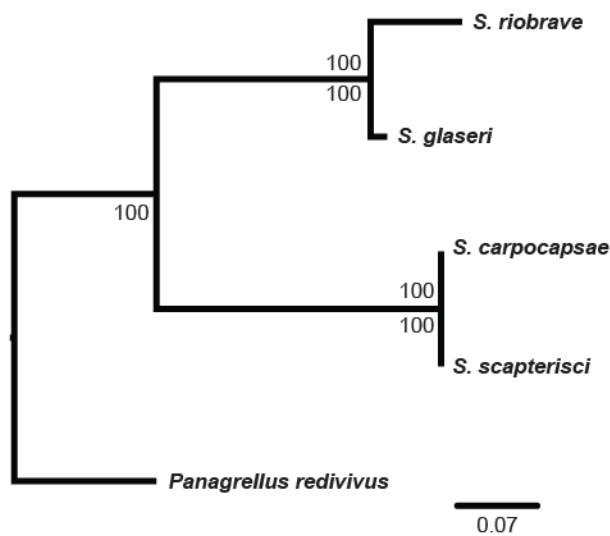
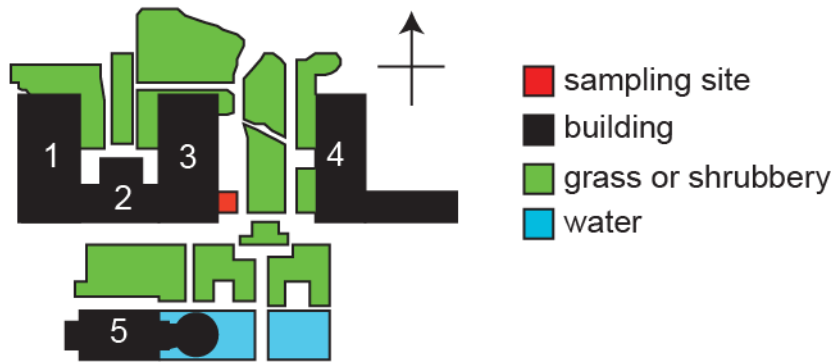


**Figure 4.S1 | Phylogeny of selected nematodes.** **A.** Phylogenetic relationships among free-living and parasitic nematodes. Relationships are based on maximum likelihood and Bayesian analyses of nearly complete SSU sequences. Values above each branch represent Bayesian posterior probabilities; ML bootstrap indices appear below each branch. Values lower than 75 are not reported. Both analyses produced concordant tree topologies. Nematode clades (1–12) are after Holterman *et al.*, 2006 [1] while clades after Blaxter *et al.*, 1998 [2] are indicated with roman numerals and colored boxes. For parasitic species, host ranges are indicated by colored icons. *Priapulid* (a priapulid) and *Chordodes* (a nematomorph) were defined as outgroups. **B.** Phylogeny of selected *Steinernema* species. Relationships are based on ML and Bayesian analysis of the large subunit ribosomal DNA. Values above each branch represent Bayesian posterior probabilities; ML bootstrap indices appear below each branch. Values lower than 75 are not reported. Both analyses produced concordant tree topologies. The tree was rooted with the free-living nematode *Panagrellus redivivus* as the outgroup species. **C.** EPNs tested. Photomicrographs of the different EPN infective juveniles (IJs), with their host-seeking strategies and host ranges.

**A** Diagram of host sampling site at Caltech



**B** Photograph of host sampling site



**Figure 4.S2 | Sampling site from which the majority of potential hosts were collected. A.** Diagram of the sampling site at Caltech. **B.** Photograph of the same sampling site. The sampling site is the small, shady grass plot visible in the foreground. Earwigs, pillbugs, and slugs were collected from the upper layers of moist soil in the vicinity of a leaky sprinkler. Flatheaded borers were collected from inside the wood of nearby rose bushes.

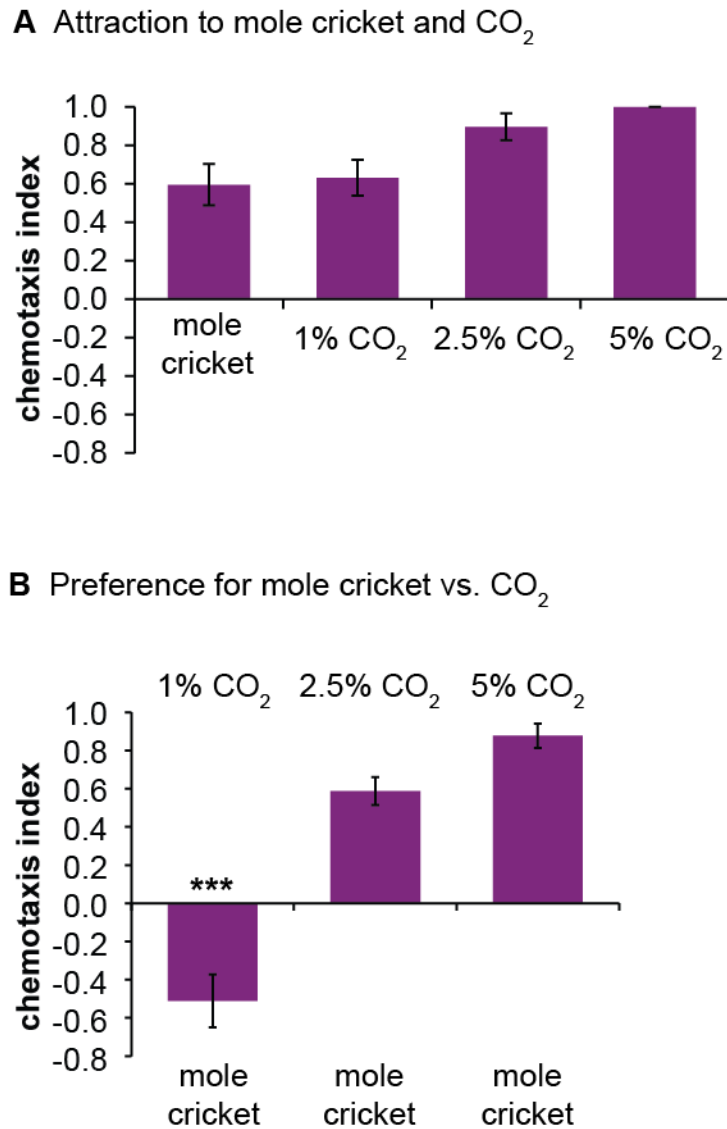
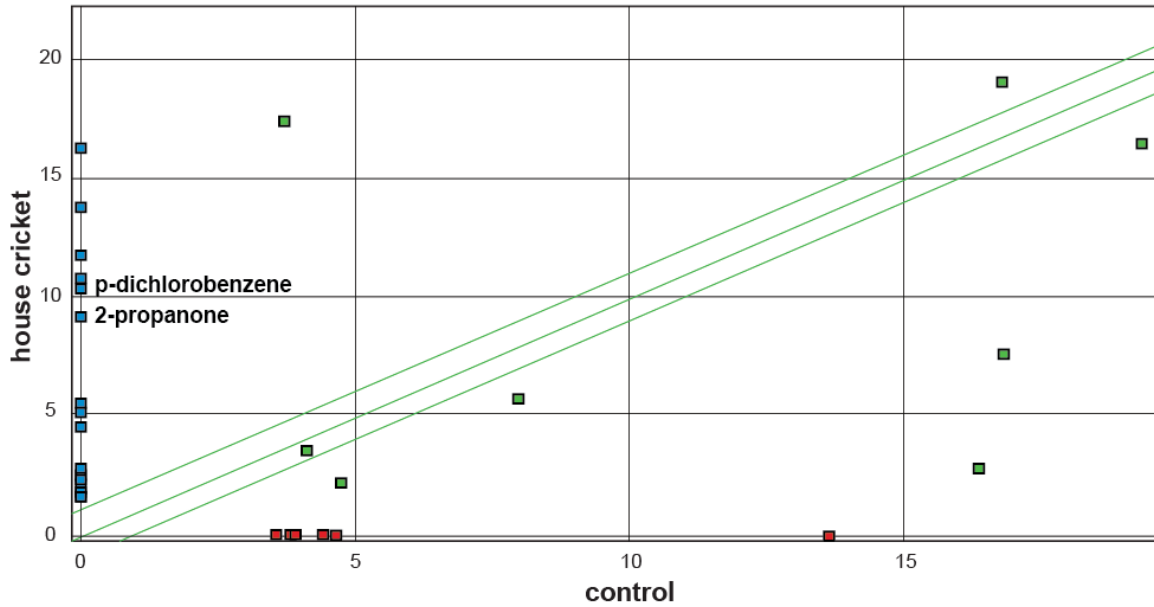


**Figure 4.S3 | Preference of *S. carpocapsae* IJs for mole cricket odor vs. CO<sub>2</sub>.** **A.** Responses of *S. carpocapsae* IJs to volatiles from an individual mole cricket and to different concentrations of CO<sub>2</sub> in a chemotaxis assay. Data are from Figs. 4.1B and 4.3A. **B.** Responses of *S. carpocapsae* IJs to volatiles from an individual mole cricket vs. different concentrations of CO<sub>2</sub> in a competition chemotaxis assay. A positive C.I. indicates attraction to CO<sub>2</sub>; a negative C.I. indicates attraction to mole cricket odor. n = 3–9 trials for each condition. The response to mole cricket odor when tested against an air control was not significantly different from the response to mole cricket odor when tested against 1% CO<sub>2</sub> (unpaired t test). The response to 1% CO<sub>2</sub> when tested against an air control was significantly different from the response to 1% CO<sub>2</sub> when tested against mole cricket odor (\*\*\*, P < 0.001); however, responses to 2.5% CO<sub>2</sub> and 5%

CO<sub>2</sub> when tested against an air control vs. mole cricket odor were not significantly different (two-factor repeated measures ANOVA).

### A SPME from house crickets



### B TD-GC-MS from mole crickets

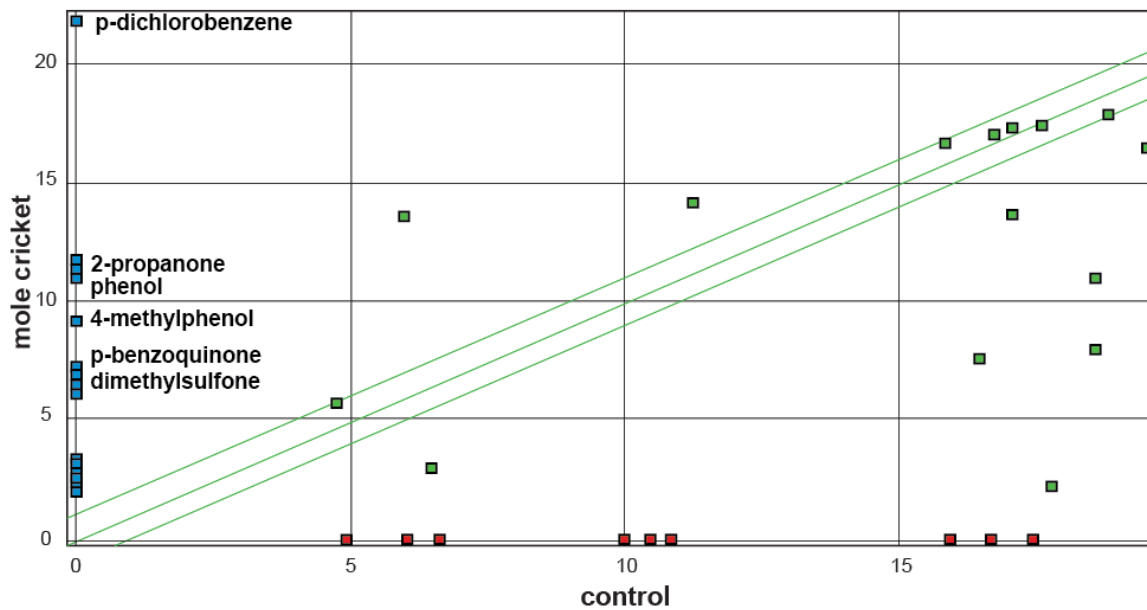
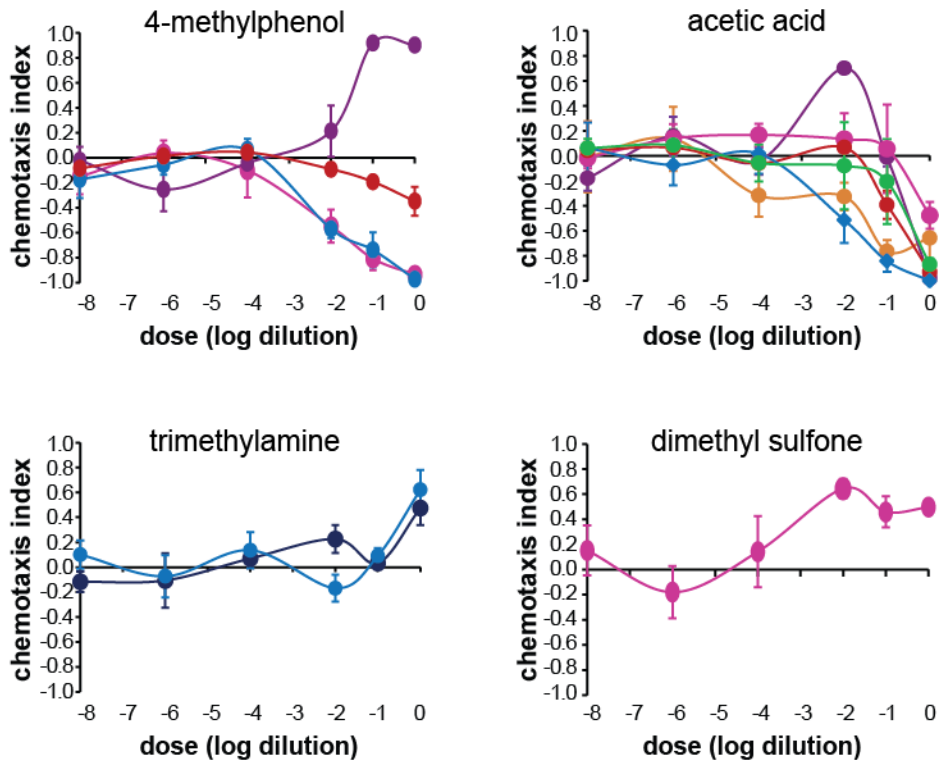


**Figure 4.S4 | Identification of host-derived odorants by GC-MS. A.** A representative trace showing SPME-GC-MS data obtained from live house crickets. **B.** A representative trace showing TD-GC-MS data obtained from live mole crickets. For both graphs, the x-axis indicates the relative abundance in control air, and the y-axis indicates relative abundance in host air. Odorants found

exclusively in host air are indicated in blue, odorants found exclusively in control air are indicated in red, and odorants found in both host air and control air are indicated in green. Of the odorants found exclusively in host air, only those identified in multiple experimental replicates at a relative abundance of  $\geq 20,000$  and with a library match of  $\geq 95\%$  confidence are labeled, with the exception of p-dichlorobenzene from house crickets, which was identified with a library match of  $\sim 90\%$ .

### A Chemotaxis across concentrations



### B Jumping across concentrations

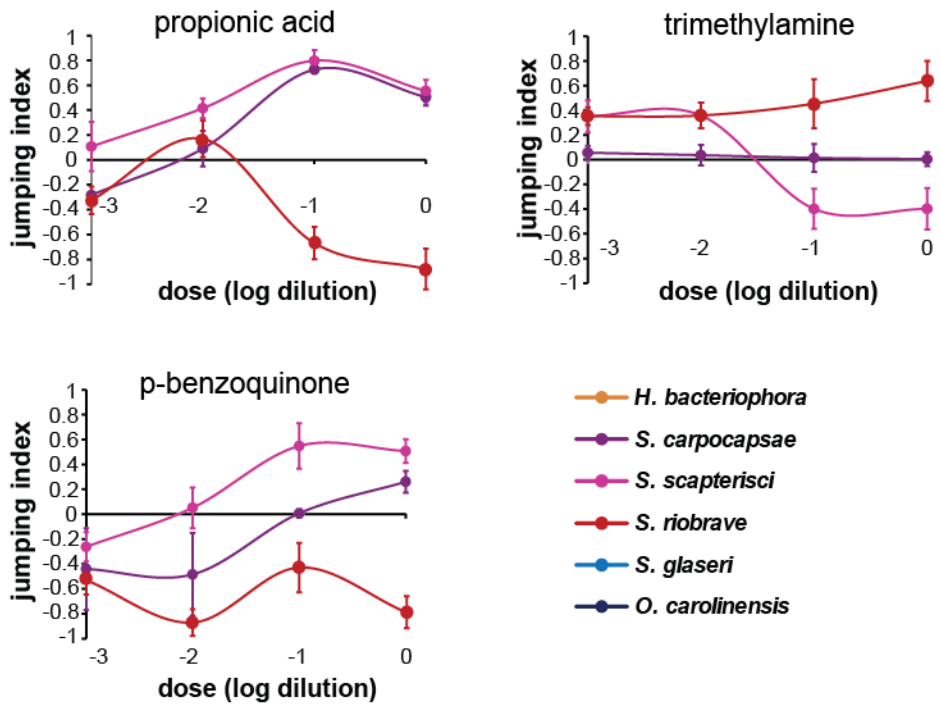


Figure 4.S5 | Dose-response analysis for selected host-derived odorants. A. Chemotaxis

behavior across concentrations. n = 4–8 trials for each EPN-odorant combination. **B.** Jumping behavior across concentrations. n = 2 trials for each EPN-odorant combination.

## **Materials and Methods**

**Nematodes.** *H. bacteriophora* were from the inbred strain M31e [3–5]. *S. carpocapsae* were from the inbred strain ALL [4, 6, 7]. *C. elegans* were the wild isolate CB4856 (“Hawaii”). *O. carolinensis* were the YEW strain [8]. *S. glaseri* were from the inbred NC strain [9]. *S. scapterisci* were inbred from the FL strain [10]. *S. riobrave* were inbred from the TX strain [11].

**Nematode culturing.** All nematodes were cultured as previously described [4]. Briefly, 5 last instar *Galleria mellonella* larvae (American Cricket Ranch, Lakeside, CA) were placed in a 5 cm Petri dish with a 55 mm Whatman 1 filter paper acting as a pseudo-soil substrate in the bottom of the dish. ≤ 250 ml containing 500–1000 IJs suspended in water was evenly distributed on the filter paper. After 7–10 days the insect cadavers were placed on White traps [12]. *Steinernema glaseri* was placed onto a modified White trap containing plaster of Paris as previously described [13]. Emerging IJs were harvested and rinsed 3 times with water. *S. scapterisci* was also cultured by infecting house crickets and mole crickets using similar techniques. IJs were stored at either room temperature or 15°C and tested within 2 months of emergence. *C. elegans* was cultured on NGM plates seeded with *E. coli* OP50 according to standard methods [14], and dauer larvae were collected from the lids of plates from which the nematodes had exhausted their bacterial food supply (i.e., “starved plates”).

**Nematode phylogeny.** Small subunit ribosomal DNA (SSU rDNA) sequences for the large phylogenetic analysis were obtained from GenBank for all taxa included in the present study (accession numbers: AJ920356, EU086375, AF036593, AY268117, U81584, AF083007,

AF279916, AF036604, AY284620, AY284621, AY284671, U94367, AF036588, U61761, AF036600, U60231, EU344798, X87984, AF036589, AF519234, AJ920348, FJ547240, AJ417024, U81581, and AF036639). A total of 23 nematode species and 2 outgroup taxa (a priapulid and a nematomorph) were used in the analyses for Figure 4.S1A. Sequences were aligned using ProAlign [15] with 1500 Mb of memory allotted, bandwidth set to 1500 with HMM model parameters being estimated from the data. We excluded characters aligned with posterior probability values under 60%, resulting in 1330 aligned characters for subsequent analysis. The TIM2+I+G model was selected as the best-fit model of substitution for all analyses using the AIC and BIC model selection criteria in the program jModelTest [16, 17]. Maximum likelihood and bootstrap (1000 replicates) analyses were carried out in PhyML 3.0 [18] using the parameters for base frequencies, substitution rate matrix, proportion of invariable sites, number of substitution categories, and shape distribution parameter determined as the best-fit by jModelTest (freqA = 0.2618, freqC = 0.1850, freqG = 0.2443, freqT = 0.3089, Ra(AC) = 1.4966, Rb(AG) = 2.4339, Rc(AT) = 1.4966, Rd(CG) = 1.0000, Re(CT) = 3.7721, Rf(GT) = 1.0000, p-inv = 0.1150, and gamma shape = 0.5290). Bayesian analysis was carried out using MrBayes 3.1.2 [19]. The number of substitution categories and shape was based on the parameters determined by jModelTest (as above). The parameters for base frequencies, relative rates, substitution rate matrix, and proportion of invariant sites were allowed to vary throughout the analysis. The parameters (shape, statefreq, and revmat) were unlinked to allow for more flexibility in searching tree space. Trees were sampled every 1000 generations. The burn-in value was set to 2000 trees. The total number of generations was set to 8 million. Four parallel chains (one cold and three heated) were used. A majority-rule consensus tree was reconstructed after discarding the burn-in.

For the four *Steinernema* species phylogeny (Figure 4.S1B), large subunit ribosomal DNA (LSU rDNA) sequences were obtained from GenBank (AF331908, AF331898, AF331893, AF331900,

and DQ145647). Sequences were aligned using ProAlign [15] with 1050 Mb of memory allotted, bandwidth set to 1000 with HMM model parameters being estimated from the data. We excluded characters aligned with posterior probability values under 60%, resulting in 883 aligned characters for subsequent analysis. The TIM3+G model was selected as the best-fit model of substitution for all analyses using both the AIC and BIC model selection criteria in the program jModelTest [16, 17]. Maximum likelihood and bootstrap (1000 replicates) analyses were carried out in PhyML 3.0 [18] using the parameters for substitution rate matrix, proportion of invariable sites, number of substitution categories, and shape distribution parameter determined as the best-fit by jModelTest (Ra(AC) = 0.3610, Rb(AG) = 1.1251, Rc(AT) = 1.0, Rd(CG) = 0.3610, Re(CT) = 3.9194, Rf(GT) = 1.0000, gamma shape = 0.5.650). Base frequencies were estimated empirically and the p-invar parameter was optimized from the data. Bayesian analysis was carried out using MrBayes 3.1.2 [19]. The number of substitution categories was based on the parameters determined by jModelTest (as above). Other parameters, such as base frequency, relative rates, substitution rate matrix, and proportion of invariant sites were allowed to vary throughout the analysis. The parameters (shape, statefreq, and revmat) were unlinked to allow for more flexibility in searching tree space. Trees were sampled every 1000 generations. The burn-in value was set to 2000 trees. The total number of generations was set to 8 million. Four parallel chains (one cold and three heated) were used. A majority-rule consensus tree was reconstructed after discarding the burn-in.

**Collection of potential hosts.** Mole crickets, earwigs, flatheaded borers, pillbugs, and slugs were collected from their natural habitats in the greater Los Angeles area and tested within a few weeks of collection. The majority of the earwigs, flatheaded borers, pillbugs, and slugs were collected from the campus of the California Institute of Technology (Figure 4.S2). Mole crickets were collected from the Rio Hondo golf course in Downey, California. Waxworms and house crickets were purchased commercially from either American Cricket Ranch or Petco®. For

potential hosts collected from natural habitats, species identities were confirmed by analysis of 18S ribosomal DNA sequence, knowledge of habitat distributions in Southern California, and analysis of diagnostic external morphological features.

**Chemotaxis assays.** Host, CO<sub>2</sub>, and odorant chemotaxis assays were performed as previously described [4]. Briefly, assays were performed on standard chemotaxis assay plates [20]. Scoring regions consisted of 2 cm diameter circles on each side of the plate along the diameter, with the center of the circle 1 cm from the edge of the plate. For host chemotaxis assays, live hosts (1 animal in the case of mole crickets, and 4–6 animals for all other hosts) were placed into a 50 ml gastight syringe, and a control syringe was filled with room air. Syringes were depressed at a rate of 0.5 ml/min using a syringe pump. Host air was delivered to one side of the assay plate and room air was delivered to the other side of the assay plate through holes drilled into the plate lids directly above the center of the scoring regions. For CO<sub>2</sub> chemotaxis assays, gastight syringes were instead filled with either a certified CO<sub>2</sub> mixture containing the test concentration of CO<sub>2</sub>, 10% O<sub>2</sub>, and the balance N<sub>2</sub>, or a control air mixture containing 10% O<sub>2</sub> and 90% N<sub>2</sub>. For odorant chemotaxis assays, 1 ml of 1 M sodium azide was placed in the center of each scoring region as an anesthetic. 5 ml of odorant was then placed in the center of one scoring region, while 5 ml of a control (either paraffin oil, dH<sub>2</sub>O, or ethanol) was placed in the center of the other scoring region. For all assays, ~ 2 ml of worm pellet containing ~ 50–150 nematodes was then placed in the center of the assay plate. Assay plates were left undisturbed on a vibration-reducing platform and scored after either 1 hour (for host and CO<sub>2</sub> chemotaxis assays) or 3 hours (for odorant assays). If at least 3 worms moved into the scoring regions, a chemotaxis index was then calculated as  $C.I. = (\# \text{ worms at CO}_2 - \# \text{ worms at air}) / (\# \text{ worms at CO}_2 + \# \text{ worms at air})$ . For the soda lime host chemotaxis assay, gas mixtures were passed through a 6 inch column

containing 2–5 mm soda lime pellets (Sigma-Aldrich 72073) before entering the assay plate, as previously described [4]. Solid odorants were dissolved as follows: 3-hydroxy-2-butanone and dimethyl sulfone, 1 g in 4 ml dH<sub>2</sub>O; 4-methylphenol and p-dichlorobenzene, 0.1 g in 5 ml paraffin oil; and p-benzoquinone, 0.1 g in 5 ml ethanol.

For the mixture assay shown in Figure 4.7A, the control assay (left bar) had 5 ml of an odorant mix containing 10<sup>-1</sup> dilutions of p-dichlorobenzene, hexanal, and  $\gamma$ -terpinene on one side of the chemotaxis plate and 5 ml of paraffin oil control on the other side. The experimental assay (right bar) had 5 ml of odorant mix containing 10<sup>-1</sup> dilutions of p-dichlorobenzene, hexanal, and  $\gamma$ -terpinene on one side of the chemotaxis plate and 5 ml of odorant mix containing 10<sup>-1</sup> dilutions of p-dichlorobenzene, hexanal,  $\gamma$ -terpinene, and 3-hydroxy-2-butanone on the other side. The soil assay shown in Figure 4.7B used a modified version of the CO<sub>2</sub> and host chemotaxis assays. For the control assay (left bar), one syringe contained 3 g of soil (collected from the sampling site shown in Figure 4.S2) and the other syringe contained air. For the experimental assay (right bar), one syringe contained 3 g of soil + 5 ml paraffin oil on a small piece of filter paper and the other syringe contained 3 g of soil + 5 ml of 4-methylphenol (dissolved as described above) on a small piece of filter paper.

**Jumping assay.** Jumping assays were performed as previously described [4]. Briefly, 100 IJs suspended in 200 ml water were evenly distributed onto a 55 mm Whatman 1 filter paper on the bottom of a 5 cm Petri dish. For host jumping assays, a single live host was placed into a 10 ml gastight syringe and a control syringe was filled with room air. For CO<sub>2</sub> jumping assays, syringes were filled with either a certified CO<sub>2</sub> mixture or air control as described above. For odorant jumping assays, a small piece of filter paper containing 5 ml of undiluted odorant was placed inside the syringe. The needle from the syringe was inserted through a 1.25 mm hole in the

side of the dish such that the tip of the needle was within  $\sim 2$  mm of a standing IJ. A small puff of air from the syringe ( $\sim 0.5$  ml volume) was then administered directly at the IJ, and a jumping response was scored if the IJ jumped within 8 s.  $\sim 20$  IJs were tested from the same arena. A normalized jumping index (J.I.) that ranged from -1 to +1 was then calculated. For stimuli that evoked higher levels of jumping than the control, the J.I. and SEM were calculated as  $J.I. = (\text{fraction jumped to stimulus} - \text{fraction jumped to control}) / (1 - \text{fraction jumped to control})$  and  $SEM = \sqrt{[(SEM \text{ for stimulus})^2 - (SEM \text{ for control})^2] / (1 - \text{fraction jumped to control})}$ . For stimuli that evoked lower levels of jumping than the control, the J.I. and SEM were calculated as  $J.I. = (\text{fraction jumped to stimulus} - \text{fraction jumped to control}) / (\text{fraction jumped to control})$  and  $SEM = \sqrt{[(SEM \text{ for stimulus})^2 - (SEM \text{ for control})^2] / (\text{fraction jumped to control})}$ . For soda lime host jumping assays, the assay setup is as described above, but gas mixtures were passed through a 2 inch column of Nalgene (8050-0250) FTP 3/16" OD tubing containing 2-5 mm soda lime pellets (Sigma-Aldrich 72073) before entering the assay arena. The column was held between 2 female-ended Swagelok compression fittings. To securely attach the column to the syringe and needle, the Swagelok fittings were filled with a male (on the needle end) and female (on the syringe end) biomedical luer fitting.

**Virulence assay.** Individual hosts were placed into either 5 cm Petri dishes (all hosts except mole crickets) or small glass baby food jars with an air hole drilled into the lid (mole crickets) containing a 55 mm Whatman 1 filter paper at the bottom. 100 IJs suspended in 200 ml water were then evenly distributed onto the filter paper. Hosts were exposed to IJs for 48 hours at room temperature, and host survival was then scored by response to gentle prodding. To assay EPN growth and reproduction in host cadavers, the cadavers were dissected at 5 days post-exposure and scored for the presence of either adult EPNs only (growth but not reproduction) or adults and

young larvae (growth and reproduction). To assay emergence from host cadavers, cadavers were placed onto standard White traps [12] at either 10 days post-exposure (all hosts except house crickets) or 5 days post-exposure (house crickets) and scored for the presence of IJs in the trap at 20 days post-exposure. For potential hosts that desiccate easily (mole crickets, house crickets, pillbugs, and slugs), 200 ml water was added to the filter paper each day to prevent desiccation.

**Identification of host-derived odorants by TD-GC-MS and SPME-GC-MS.** TD-GC-MS was performed as previously described [4]. TD-GC-MS data for waxworms and house crickets was from Hallem et al., 2011 [4]. Both the collection of volatile organic compounds (VOCs) and subsequent solid phase microextraction (SPME) analysis were modified from Villaverde et al., 2007 [21]. Briefly, VOCs were collected for SPME analysis by placing insects into 10 ml glass vials, sealed with a Teflon septum (SUPLECO 27529). The larger and potentially cannibalistic insects (mole crickets and house crickets) were placed individually into sampling vials whereas all other, smaller species (waxworms, flat-headed borers, pillbugs, and earwigs) were sampled with four individuals per sampling vial. Experiments were done in pairs and replicated 3 times, with an empty control sampling vial being run each time. Clean, sterile vials were used each time. After 12 hrs, volatiles secreted were sampled from the head space, corresponding to the gaseous phase in contact with the insect sample. VOCs were sampled for 15 minutes using carboxen/polydimethylsiloxane (CAR/PDMS) fiber (75 mm film thickness) (SUPELCO 504831). Selection of fibers was based on manufacturer's recommendations for sampling volatiles of low to intermediate polarity and from data reported by Villaverde et al., 2007 [21]. Fibers were preconditioned in accordance with the manufacturer's instructions. Quantitative analysis was performed using a Hewlett Packard 6890 GC-5973 MS gas chromatograph-mass spectrometer (Agilent Technologies, US) employing a non-polar DB-5 capillary column (30m x 0.25mm, 0.25 micron film thickness) (Agilent). The injector was operated in the splitless mode at 250°C and

the oven temperature was programmed (40°C for 3 min, 5°C/min to 80°C, 20°C/min to 150°C, and 30°C/min to 250°C, with a holding time of 10 min at the final temperature). The transfer line temperature was set at 280°C and the ion source was held at 250°C. VOC identification was performed by CGC–MS analysis with an Eclipse 4660 purge and trap sampler with chromatographic conditions similar to the CGC; the ion source was set at 200°C and the transfer line at 275°C. VOC were tentatively identified by interpretation of their mass spectral fragmentation. Data was analyzed with both Chemstation and Masshunter software. Mass spectra were also compared to data from the Wiley library (275,000 spectra) of electron impact mass spectra. Only compounds that were found in multiple traces ( $\geq 2$ ) with a relative abundance  $\geq 20,000$ , were not present in the control traces, and had library matches of  $\geq 95\%$  were considered in this study.

**Data analysis.** Statistical analysis was performed using either GraphPad InStat, GraphPad Prism, or PAST [22]. Two-factor ANOVAs with Bonferroni post-tests were used to compare the responses of the different EPNs to the different hosts or host-derived odorants. *P* values from the ANOVAs (factor 1, factor 2, and the interaction between the factors) are given in the figure legends; *P* values from the post-tests are given in the supplemental tables. For example, when examining the responses of the different EPNs to the different hosts, we show that EPNs respond differently to different hosts ( $P < 0.0001$  for factor one), different hosts evoke different overall responses from EPNs ( $P < 0.0001$  for factor two), and different EPNs show different odor response profiles ( $P < 0.0001$  for the interaction). Heatmaps were generated using Heatmap Builder [23].

**Supplemental Data.** The original published version of this work, Dillman et al. [24], has 14 supplemental data sets associated with it. Those data sets are available online (<http://www.pnas.org/content/109/35/E2324/suppl/DCSupplemental>).

1. Holterman, M., van der Wurff, A., van den Elsen, S., van Megen, H., Bongers, T., Holovachov, O., Bakker, J., and Helder, J. (2006). Phylum-wide analysis of SSU rDNA reveals deep phylogenetic relationships among nematodes and accelerated evolution toward crown clades. *Molecular Biology and Evolution* 23, 1792–1800.
2. Blaxter, M.L., De Ley, P., Garey, J.R., Liu, L.X., Scheldeman, P., Vierstraete, A., Vanfleteren, J.R., Mackey, L.Y., Dorris, M., Frisse, L.M., et al. (1998). A molecular evolutionary framework for the phylum Nematoda. *Nature* 392, 71–75.
3. Ciche, T.A., Kim, K.S., Kaufmann-Daszczuk, B., Nguyen, K.C., and Hall, D.H. (2008). Cell invasion and matricide during *Photorhabdus luminescens* transmission by *Heterorhabditis bacteriophora* nematodes. *Applied and environmental microbiology* 74, 2275–2287.
4. Hallem, E.A., Dillman, A.R., Hong, A.V., Zhang, Y., Yano, J.M., DeMarco, S.F., and Sternberg, P.W. (2011). A sensory code for host seeking in parasitic nematodes. *Current Biology* 21, 377–383.
5. Hallem, E.A., Rengarajan, M., Ciche, T.A., and Sternberg, P.W. (2007). Nematodes, bacteria, and flies: a tripartite model for nematode parasitism. *Current biology: CB* 17, 898–904.
6. Bilgrami, A.L., Gaugler, R., Shapiro-Ilan, D.I., and Adams, B.J. (2006). Source of trait deterioration in entomopathogenic nematodes *Heterorhabditis bacteriophora* and *Steinernema carpocapsae* during *in vivo* culture. *Nematology* 8, 397–409.
7. Chaston, J.M., Dillman, A.R., Shapiro-Ilan, D.I., Bilgrami, A.L., Gaugler, R., Hopper, K.R., and Adams, B.J. (2011). Outcrossing and crossbreeding recovers deteriorated traits in laboratory cultured *Steinernema carpocapsae* nematodes. *Int J Parasitol* 41, 801–809.
8. Ye, W.M., Torres-Barragan, A., and Cardoza, Y.J. (2010). *Oscheius carolinensis* n. sp (Nematoda: Rhabditidae), a potential entomopathogenic nematode from vermicompost. *Nematology* 12, 121–135.
9. Li, X., Cowles, E.A., Cowles, R.S., Gaugler, R., and Cox-Foster, D.L. (2009). Characterization of immunosuppressive surface coat proteins from *Steinernema glaseri* that selectively kill blood cells in susceptible hosts. *Molecular and biochemical parasitology* 165, 162–169.
10. Nguyen, K.B., and Smart, G.C. (1991). Pathogenicity of *Steinernema scapterisci* to Selected Invertebrates. *J. Nematol.* 23, 7–11.
11. Canhilal, R., Reid, W., Kutuk, H., and El-Bouhssini, M. (2007). Susceptibility of Sunn Pest, *Eurygaster integriceps* Puton (Hemiptera: Scutelleridae), to Various Entomopathogenic Nematodes (Rhabditida: Steinernematidae and Heterorhabditidae). *J Agr Urban Entomol* 24, 19–26.

12. White, G.F. (1927). A Method for Obtaining Infective Nematode Larvae from Cultures. *Science* 66, 302–303.
13. Kaya, H.K., and Stock, S.P. (1997). Techniques in insect nematology. In *Manual of techniques in insect pathology*, L. Lacey, ed. (San Diego, CA: Academic Press Limited).
14. Brenner, S. (1974). The genetics of *Caenorhabditis elegans*. *Genetics* 77, 71–94.
15. Loytynoja, A., and Milinkovitch, M.C. (2003). A hidden Markov model for progressive multiple alignment. *Bioinformatics* 19, 1505–1513.
16. Guindon, S., and Gascuel, O. (2003). A simple, fast, and accurate algorithm to estimate large phylogenies by maximum likelihood. *Syst Biol* 52, 696–704.
17. Posada, D. (2009). Selection of models of DNA evolution with jModelTest. *Methods Mol Biol* 537, 93–112.
18. Guindon, S., Dufayard, J.F., Lefort, V., Anisimova, M., Hordijk, W., and Gascuel, O. (2010). New algorithms and methods to estimate maximum-likelihood phylogenies: Assessing the performance of PhyML 3.0. *Systematic Biology* 59, 307–321.
19. Huelsenbeck, J.P., and Ronquist, F. (2001). MRBAYES: Bayesian inference of phylogenetic trees. *Bioinformatics* 17, 754–755.
20. Bargmann, C.I., Hartweg, E., and Horvitz, H.R. (1993). Odorant-selective genes and neurons mediate olfaction in *C. elegans*. *Cell* 74, 515–527.
21. Villaverde, M.L., Juarez, M.P., and Mijailovsky, S. (2007). Detection of *Tribolium castaneum* (Herbst) volatile defensive secretions by solid phase micro extraction-capillary gas chromatography (SPME-CGC). *J Stored Prod Res* 43, 540–545.
22. Hammer, Ø., Harper, D.A.T., and Ryan, P.D. (2001). PAST: Paleontological Statistics Software Package for Education and Data Analysis. *Palaeontol Electronica* 4, 9.
23. King, J.Y., Ferrara, R., Tabibiazar, R., Spin, J.M., Chen, M.M., Kuchinsky, A., Vailaya, A., Kincaid, R., Tsalenko, A., Deng, D.X., et al. (2005). Pathway analysis of coronary atherosclerosis. *Physiological genomics* 23, 103–118.
24. Dillman, A.R., Guillermin, M.L., Lee, J.H., Kim, B., Sternberg, P.W., and Hallem, E.A. (2012). Olfaction shapes host-parasite interactions in parasitic nematodes. *Proc Natl Acad Sci U S A* 109, E2324–2333.